

# The Application of Optimisation Algorithms in Antenna Array Beampattern Synthesis

Jonathan D. Gorman

School of Electrical, Electronic and Communications Engineering

University College Dublin

Belfield, Dublin 4, Ireland.

*jonathan.gorman@ucdconnect.ie*

**Abstract**—In this paper, optimisation algorithms are successfully applied to a number of antenna array beampattern synthesis problems – including, a Uniform Linear Array (ULA), a ULA with an inactive element, and a 2D Wireless Sensor Network (WSN) array. The algorithms presented include a Greedy Algorithm (GDA), a Metropolis Algorithm (MA), and a Genetic Algorithm (GA).

**Keywords**—antenna array beampattern synthesis, optimisation algorithm, uniform linear array, wireless sensor network, greedy algorithm, metropolis algorithm, genetic algorithm, collaborative beamforming, Dolph-Chebyshev, internet of things.

## I. INTRODUCTION

The ubiquitous Internet of Things (IoT) paradigm is expected to see the number of physical objects connected to the internet increase significantly into the 21<sup>st</sup> century [1]. A key component of the IoT is the Wireless Sensor Network (WSN), which will involve clusters of spatially distributed autonomous sensor nodes being used to monitor and sense physical changes in a variety of scenarios. The combination of the IoT and WSNs will allow for increased sensor communication and collaboration via the internet [2].

However, small sensor batteries are often neither replaceable nor rechargeable which can lead to issues surrounding a sensor's energy autonomy. This can have a detrimental effect on the overall lifetime of a WSN. The extension of a sensor's battery life is therefore a matter of great interest, with concepts such as energy harvesting [3], and routing algorithms [4] having been shown to prolong the battery life of a sensor.

The technique focused on in this paper is Collaborative Beamforming (CB), a process whereby multiple nodes collaborate in order to form a distributed sensor array and following data acquisition and sharing amongst all nodes, transmit in the desired direction in a way such that constructive interference occurs at the receiver (Fig. 1). CB can result in energy savings for all sensors involved in the network through the sharing of the transmission overhead, thus improving the lifetime of the network. Further positives include increased transmission range, as well as improved data security by minimising signals in unintended directions. Promising results, as illustrated in [5] and [6] showed overall network lifetime improvements using CB concepts.

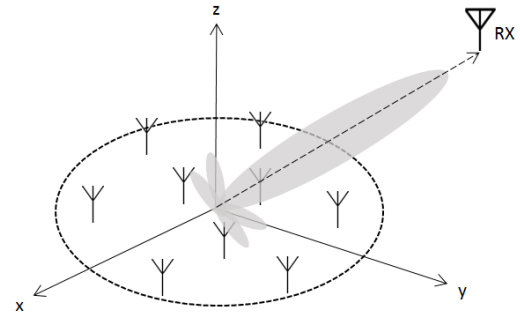


Fig.1. A diagram illustrating collaborative beamforming via a distributed Wireless Sensor Network array with an example radiation beampattern in the direction of a receiver.

### A. Array Beampattern Synthesis Characteristics

A lot of emphasis is placed on optimising an antenna's array beampattern. This beampattern is characterised by a Main Lobe (ML), a number of Side Lobes (SL), a Side Lobe Level (SLL) and a Beam Width (BW) which allow for visualisation as to where an antenna transmits or receives power (Fig. 2). It is widely accepted that it is generally desirable to compress the BW and also minimise the SLL as they represent radiation in unintended directions, which indicates power loss [7]. The beampattern produced by an array is dependent on the current feeding each of the elements.

This synthesis problem is well documented in literature as a result of its application in many communications technologies. One of the original papers on the topic of array pattern synthesis was produced by Dolph [8] who introduced a prominent result in this field which showed an optimisation of the relationship between the BW and SLL. The proposed method provided an excitation current distribution for a phased Uniform Linear Array (ULA) which resulted in a beampattern in which all SLs are at the same level and the BW was minimised.

It is also shown in [8] that in order to achieve low SLs some sacrifices to the overall gain and BW are required. This provides, what is often termed the minimax response and is acceptable in many applications. This method which was based on Chebyshev polynomials is often cited in literature as the Dolph-Chebyshev (D-C) method and is widely accepted as yielding the optimal array pattern for ULAs [9].

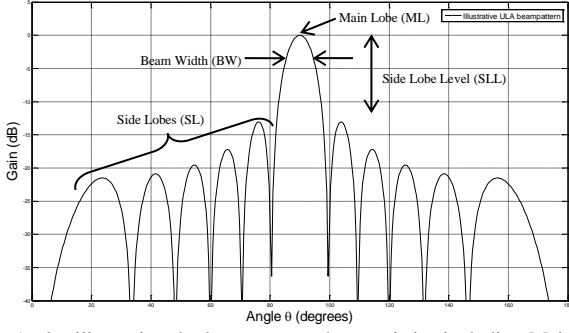


Fig.2. A plot illustrating the beam pattern characteristics including Main Lobe, Side Lobes, Side Lobe Level and Beam Width.

The synthesis procedure outlined in this paper applies a number of optimisation algorithms which aim to find a current excitation vector  $\vec{I}$  which when applied to the array elements of three test cases, minimises a quantity known as the Beam Ratio (BR) – which is the ratio of the SLL to the ML. This paper uses the value of the BR to quantify the extent of optimisation.

## II. UNIFORM LINEAR ARRAY MODELS

The ULA model consists of  $N$  isotopically radiating elements uniformly spaced in a line (Fig. 3). The inter-element spacing is  $d$  (wavelengths), the angle made with the x-axis is  $\theta_k$  (degrees), the current applied to a specific array element is  $I_n$ , and  $\psi$  is the progressive phase difference. All elements are assumed to be perfect isotropic radiators and channel effects such reflection, fading, scattering, etc. are ignored.

The far-field pattern for the first element ( $n = 0$ ) of the ULA in an initial direction of  $0^\circ$  is given by

$$E_0 = I_0 e^{j(2\pi \cos(\theta_0) + \psi)} \quad (1)$$

The combined pattern produced by an array for a given set of angles  $\theta_k$  is a sum of all components and is defined as

$$E(\theta_k) = \sum_{n=0}^{N-1} I_n e^{jn(2\pi \cos(\theta_k) + \psi)} \quad (2)$$

Equation (2) is vectorised, such that a matrix of phasors is multiplied by a variable excitation vector. This is given as follows:

$$\begin{bmatrix} E(\theta_1) \\ E(\theta_2) \\ \vdots \\ E(\theta_k) \end{bmatrix} = \begin{bmatrix} e^{j0(2\pi \cos(\theta_1) + \psi)} & e^{j1(2\pi \cos(\theta_1) + \psi)} & \dots & e^{jn(2\pi \cos(\theta_1) + \psi)} \\ e^{j0(2\pi \cos(\theta_2) + \psi)} & e^{j1(2\pi \cos(\theta_2) + \psi)} & \dots & e^{jn(2\pi \cos(\theta_2) + \psi)} \\ \vdots & \vdots & \ddots & \vdots \\ e^{j0(2\pi \cos(\theta_k) + \psi)} & e^{j1(2\pi \cos(\theta_k) + \psi)} & \dots & e^{jn(2\pi \cos(\theta_k) + \psi)} \end{bmatrix} \begin{bmatrix} I_1 \\ I_2 \\ \vdots \\ I_n \end{bmatrix} \quad (3)$$

The first test case is a 12 element ULA with an inter-element spacing  $d$  equal to 0.5 wavelengths. The initial current applied to each of the array elements is unity and the progressive phase difference  $\psi$  is equal to zero. The beam pattern is analysed for angles between  $0^\circ$  and  $180^\circ$ .

The second case is a duplicate of the first ULA case, but with element 6 inactive. Notably, element 6 is in a prominent position of the ULA and has the most detrimental effect on the array's performance. The initial excitation vector applied is again unity, except for the inactive element which remains at 0.

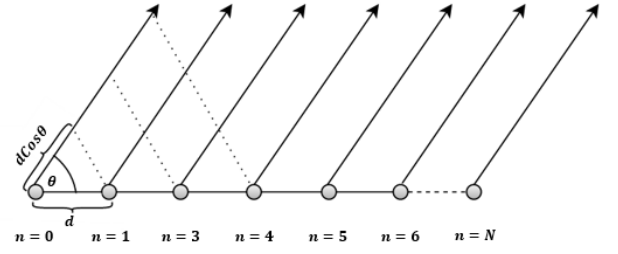


Fig.3. A diagram outlining the Uniform Linear Array model with  $N$  isotopically radiating elements uniformly spaced in a line.

Research into arrays with missing/broken elements has been completed in [10] [11] and [12]. However, this paper outlines the first application of this specific set of optimisation algorithms to aid this particular problem.

## III. 2D WIRELESS SENSOR NETWORK ARRAY MODEL

This model utilises  $N$  sensors randomly scattered in a circular 2D network of a specified radius expressed in wavelengths (Fig.4). The combined far-field pattern of the array elements can be found similarly to (2), but where the radius  $r_n$  and angle  $\phi_n$  represent the polar coordinates of the sensors in the network. The current applied to a specific array element is again  $I_n$ . This is represented by

$$E(\theta_k) = \sum_{n=0}^{N-1} I_n e^{-j2\pi r_n \cos(\theta_k - \phi_n)} \quad (4)$$

Equation (4) was also vectorised, such that the following expression was found:

$$\begin{bmatrix} E(\theta_1) \\ E(\theta_2) \\ \vdots \\ E(\theta_k) \end{bmatrix} = \begin{bmatrix} e^{-j2\pi r_1 \cos(\theta_1 - \phi_1)} & e^{-j2\pi r_2 \cos(\theta_1 - \phi_2)} & \dots & e^{-j2\pi r_n \cos(\theta_1 - \phi_n)} \\ e^{-j2\pi r_1 \cos(\theta_2 - \phi_1)} & e^{-j2\pi r_2 \cos(\theta_2 - \phi_2)} & \dots & e^{-j2\pi r_n \cos(\theta_2 - \phi_n)} \\ \vdots & \vdots & \ddots & \vdots \\ e^{-j2\pi r_1 \cos(\theta_k - \phi_1)} & e^{-j2\pi r_2 \cos(\theta_k - \phi_2)} & \dots & e^{-j2\pi r_n \cos(\theta_k - \phi_n)} \end{bmatrix} \begin{bmatrix} I_1 \\ I_2 \\ \vdots \\ I_n \end{bmatrix} \quad (5)$$

The test case has 32 elements in a circle of radius 4 wavelengths. The initial excitation vector  $\vec{I}$  applied was equal to the conjugate of the phasors corresponding to the direction in which the beam was to be steered. This is such that the beam was steered at  $180^\circ$  to the x-axis, as per the mock receiver's position in Fig. 4. The value of  $\psi$  is equal to zero. The applied set of optimisation algorithms to the case of the 2D WSN is the first documented application in the field.

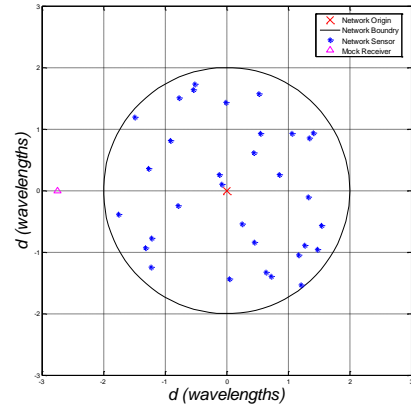


Fig.4. Plot of randomly generated 32 element Wireless Sensor Network array of radius 4 wavelengths, including mock receiver at  $180^\circ$ .

#### IV. ALGORITHM IMPLEMENTATION

Optimisation algorithms are applied to the antenna array models using MATLAB as the simulation environment. The initial excitation vector  $\vec{I}$  is applied to the array's elements following which; the corresponding BR of the beampattern is calculated. This BR value is set as the value of the initial Cost Function (CF), which is minimised.

$$\text{Cost Function} = \text{Beam Ratio} \quad (6)$$

Each algorithm follows a similar process, as outlined in Fig. 5. The aim is to minimise the CF consisting of the BR of the current beampattern. This involves an iterative process whereby the excitation vector  $\vec{I}$  is continuously varied, while monitoring the corresponding value of the CF. Each of the algorithms presented differ primarily in their variation of the excitation vector  $\vec{I}$  which leads to varying convergence times and quality of the final solution. The algorithms vary the current excitation vector varied according to changes in the CF until a maximum number of iterations are reached. Following completion, a more optimum excitation vector is obtained.

In order to ensure that sufficient comparisons between each of the algorithms can be constructed, the initial beampattern and corresponding initial CF value in each of the test cases was used as a starting point for the algorithms outlined. The time period that the algorithms were run for is also kept constant at 2000 sec.

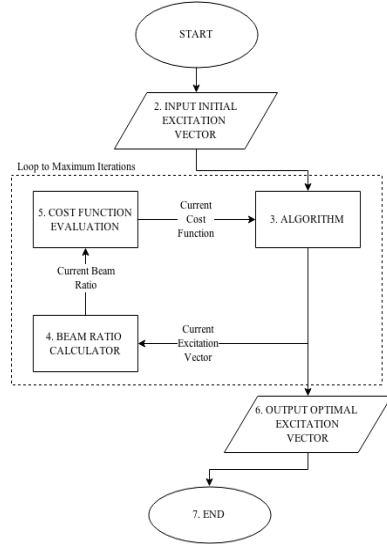


Fig.5. A flowchart outlining the process taken by all algorithms

#### V. GREEDY ALGORITHM

The Greedy Algorithm (GDA) implemented is a search heuristic that employs a scheme by which the locally optimal choice is made at each stage. This process is characterized by generally, not producing a globally optimal solution; but instead, a locally optimal solution as a result of its ‘non-reversible’ nature.

A random Gaussian perturbation is added to each element of the excitation vector at each iteration in an attempt to minimise the CF. The corresponding CF is determined and the perturbed excitation vector is stored if it has led to a decrease in the value of CF, otherwise it is discarded. The magnitude of the perturbations added to the excitation vector is determined by a parameter  $\sigma$  which decreases in size according to the number of iterations completed. The variation of the perturbation vector via the  $\sigma$  parameter allows for fine tuning of the excitation vector, which can lead to further increases in the CF. The stopping condition is a time limit of 2000 seconds.

#### VI. METROPOLIS ALGORITHM

A Metropolis Algorithm (MA), as first proposed by Metropolis [13], is also applied to the problem cases. This algorithm operates similarly to the GDA outlined, but acts according to a temperature profile. At a high temperature the algorithm has a higher probability of accepting Gaussian random perturbations added to the current excitation vector which does not lead to a lower CF. However, as the temperature drops the probability of acceptance also drops. This leads to the algorithm behaving like the GDA at lower temperatures.

The temperature profile also introduces an ‘exploration’ property which attempts to remove the possibility of the algorithm converging to a local minimum which may overlook more optimal solutions in the surrounding search space. The temperature profile is dictated by the  $\alpha$  variable

$$\alpha = \frac{m}{\sqrt{T_{final}}} \quad (7)$$

where  $m$  is the maximum number of iterations  $T_{final}$  is the final temperature value. This variable  $\alpha$  given in (7) directly affects the probability of acceptance of the algorithm given by

$$\mathbb{P}(\text{acceptance}) = e^{-\frac{\Delta CF}{T_m \alpha}} \quad (8)$$

where  $\Delta CF$  is the difference between the optimum and the current excitation vector and  $T_m$  is the temperature at the current iteration  $m$ . The temperature at each iteration  $T_m$  is also used to control the magnitude of the added random Gaussian perturbations. The algorithm proceeds until it reaches the specified time limit of 2000 seconds.

#### VII. GENETIC ALGORITHM

The Genetic Algorithm (GA) is a global search heuristic that mimics natural selection and other biological processes. The GA applied is provided by MATLAB’s Optimisation Toolbox [14]. The algorithm begins in the first generation by creating a random initial population consisting of a variety of current excitation vectors. The following populations are created using the individuals of the previous generations, having assessed their contribution to the minimisation of the CF – this is known as an individual’s fitness value.

Having assessed the fitness of a generation, the GA creates three groups of children which progress to the next generation – Elite Children (EC), Crossover Children (CC), and Mutation Children (MC). The EC are comprised of the best individuals from the current generation in terms of their fitness value. The CC are created by combining a pair of individuals from the current generation. The remaining individuals of the next generation are MC, which are randomly perturbed individuals from the current generation. The combination of EC, CC and MC are the initial population of the next generation. The algorithm progresses through generations as the current excitation vector ‘evolves’ towards an optimum solution to the problem. The GA in all cases runs for a maximum of 2000 seconds.

## VIII. SIMULATION RESULTS

### A. Results of 12 Element ULA Case

The algorithms are found to be extremely effective in optimising the 12 element ULA’s beampattern over the 2000 second time period. Notably, the resultant beampattern is similar in nature to the beampattern outlined by Dolph in [8]. This is illustrated in Fig. 6 where the three optimised beampatterns are compared with the initial beampattern. This indicates that each of the algorithms presented are capable of providing close to the known optimum solution in the case of the ULA.

Table I outlines the optimised beampattern characteristics for the 12 Element ULA test case. The MA is found to be the most effective in providing an excitation vector which minimises the BR in the given time period. The MA provides a decrease of -7.03 dB from the initial max SL. The second most effective algorithm is the GDA and thirdly, the GA. Although the minimised BRs vary, the value obtained in each of the three cases is acceptable as it shows a significant improvement on the array’s initial beampattern.

TABLE I. TABLE OF RESULTS FOR 12 ELEMENT ULA

Algorithm	Max SL* (dB)	BR	Time (sec)	Iterations/Generations
Initial	-13.06	0.2223	N/A	N/A
GDA	-19.84	0.1018	2000	1,006,114
MA	-20.09	0.0989	2000	24,358,159
GA	-19.21	0.1096	2000	828,169

\*The Max SL value in dB is with respect to the ML

### B. Results of 12 Element ULA with Element 6 Inactive Case

The prominent position of inactive element number 6 undoubtedly makes the optimisation process more difficult in this case. The resulting optimised beampattern characteristics as given in Table II show a decrease in the BR in the region of 50% - varying slightly according to the optimisation algorithm used.

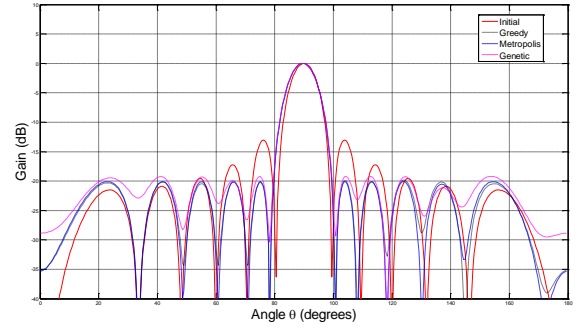


Fig.6. A plot comparing the optimised results of the 12 element ULA with element 6 inactive using the Greedy, Metropolis and Genetic algorithms

Similarly to Table I, the MA provides the lowest BR value over the given time period which results max SL value -5.882 dB down from the initial max SL. Both the GDA and GA also show improvements in the BR value with max SL reductions of -5.502 and -5.432 respectively from the initial max SL. A plot comparing the optimised beampatterns and the initial beampattern can be seen in Fig.7.

The results given in Table II indicate that the application of the GDA, MA and GA are capable of providing current excitations in the case of an array element failure. As well as this, it should be noted that optimising the array with an inactive element is capable of optimising the beampattern such that a BR value lower than the original array when all elements are active is found. This is demonstrated by the max SL in Table II which is -2.49 dB down from the initial max SL given in Table I.

TABLE II. TABLE OF RESULTS FOR 12 ELEMENT ULA WITH INACTIVE ELEMENT NUMBER 6

ALGORITHM	Max SL* (dB)	BR	Time (sec)	Iterations/Generations
Initial	-9.668	0.3286	N/A	N/A
GDA	-15.17	0.1743	2000	998,991
MA	-15.55	0.1669	2000	29,363,873
GA	-15.10	0.1758	2000	334,325

\*The Max SL value in dB is with respect to the ML

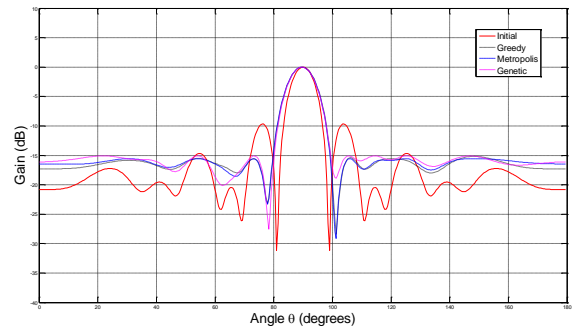


Fig.7. A plot comparing the optimised results of the 12 element ULA with element 6 inactive using the Greedy, Metropolis and Genetic algorithms.

### C. Results of 2D Wireless Sensor Network Array Model with 32 Elements Case

The random placement of the 32 sensors in the sensor array ensures that the initial beampattern is highly asymmetric in nature. This provides a more significant optimisation challenge than the two previous cases outlined. A comparison of the optimised beampattern when compared with the initial beampattern (Fig.8) indicates that the optimisation algorithms are all capable of successfully minimising to the BR. The exact figures are provided in Table III.

On average, the results in Table III indicate a reduction of -13.41 dB from the initial max SL was found. Again, and similar as in the previous test cases, the application of the MA provides an excitation vector which yields the lowest value of BR at 0.0663 in the given time limit. The GA and the GDA are also successful in optimising the antenna's beampattern yielding BRs of 0.1690 and 0.0571. However, the GDA is more successful than the GA in the given time limit.

### IX. CONCLUSION

The results outlined in this paper demonstrate the effectiveness and flexibility of the applied optimisation algorithms in a number of antenna beampattern synthesis problems. The results also indicate that the MA is more effective than GDA and GA. The reduction in the beampattern's BR value in each of the cases, relates directly to a decrease in the radiated energy in unintended directions which ultimately leads to a reduction in energy loss. The energy savings may be highly instrumental in extending the network lifetime of a WSN – a key component of the IoT concept.

TABLE III. TABLE OF RESULTS FOR 32 ELEMENT WIRELESS SENSOR NETWORK ARRAY

Algorithm	Max SL (dB)	BR	Time (sec)	Iterations/Generations
Initial	-6.886	0.4531	N/A	N/A
GDA	-24.87	0.0571	2000	10,449,782
MA	-23.58	0.0663	2000	11,498,890
GA	-15.44	0.1690	2000	436,492

\*The Max SL value in dB is with respect to the ML

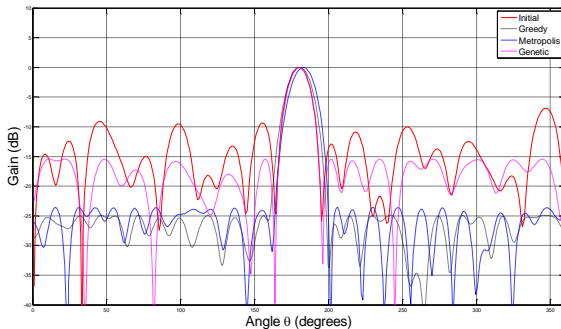


Fig.8. A comparison plot outlining the optimised the 32 element 2D WSN array using the Greedy, Metropolis and Genetic algorithms.

### REFERENCES

- [1] D. Evans, "The Internet of Things: How the Next Evolution of the Internet Is Changing Everything" 1 April 2011. [Online]. Available: [http://www.cisco.com/web/about/ac79/docs/innov/IoT\\_IBSG\\_0411FIN\\_AL.pdf](http://www.cisco.com/web/about/ac79/docs/innov/IoT_IBSG_0411FIN_AL.pdf). [Accessed 16 03 2015].
- [2] C. Alcaraz, P. Najera, J. Lopez, R. Roman "Wireless Sensor Networks and the Internet of Things: Do We Need a Complete Integration?," in 1st International Workshop on the Security of the Internet of Things (SecIoT'10), Tokyo, 2010.
- [3] Shaobo Mao; Man Hon Cheung; Wong, V.W.S., "An optimal energy allocation algorithm for energy harvesting wireless sensor networks," Communications (ICC), 2012 IEEE International Conference on , vol., no., pp.265,270, 10-15 June 2012.
- [4] Jing Feng; Nimmagadda, Y.; Yung-Hsiang Lu; Byunghoo Jung; Peroulis, D.; Hu, Y.C., "Analysis of Energy Consumption on Data Sharing in Beamforming for Wireless Sensor Networks," Computer Communications and Networks (ICCCN), 2010 Proceedings of 19th International Conference on , vol., no., pp.1,6, 2-5 Aug. 2010.
- [5] Han, Z.; Poor, H.V., "Lifetime improvement in wireless sensor networks via collaborative beamforming and cooperative transmission," Microwaves, Antennas & Propagation, IET , vol.1, no.6, pp.1103,1110, Dec. 2007.
- [6] Jing Feng; Yung-Hsiang Lu; Byunghoo Jung; Peroulis, D., "Energy efficient collaborative beamforming in wireless sensor networks," Circuits and Systems, 2009. ISCAS 2009. IEEE International Symposium on , vol., no., pp.2161,2164, 24-27 May 2009.
- [7] Ahmed, M.F.A.; Vorobyov, S.A., "Node selection for sidelobe control in collaborative beamforming for wireless sensor networks," Signal Processing Advances in Wireless Communications, 2009. SPAWC '09. IEEE 10th Workshop on , vol., no., pp.519,523, 21-24 June 2009.
- [8] Dolph, C.L., "A Current Distribution for Broadside Arrays Which Optimizes the Relationship between Beam Width and Side-Lobe Level," Proceedings of the IRE , vol.34, no.6, pp.335,348, June 1946.
- [9] Zhou, P.Y.; Ingram, M.A.; Anderson, P.D., "Synthesis of minimax sidelobes for arbitrary arrays," Antennas and Propagation, IEEE Transactions on , vol.46, no.11, pp.1759,1760, Nov 1998.
- [10] Cui Lin; Yaan Li, "The method research of beamforming with array-element failure," Computer, Mechatronics, Control and Electronic Engineering (CMCE), 2010 International Conference on , vol.1, no., pp.111,114, 24-26 Aug. 2010.
- [11] Minghui Li; McGuire, M.; Kwok Shun Ho; Hayward, G., "Array element failure correction for robust ultrasound beamforming and imaging," Ultrasonics Symposium (IUS), 2010 IEEE , vol., no., pp.29,32, 11-14 Oct. 2010.
- [12] Taskin, Aydiner; Gurel, Cigdem Seckin, "Antenna Array Pattern Optimisation In The Case Of Array Element Failure," Microwave Conference, 2003. 33rd European , vol., no., pp.1083,1085, Oct. 2003.
- [13] N. Metropolis and S. Ulam, "The Monte Carlo Method," Journal of the American Statistical Association, vol. 44, no. 247, pp. 335-341, 1949.
- [14] MathWorks, "Documentation - Global Optimisation toolbox," MathWorks, 19 03 2015. [Online]. Available: <http://uk.mathworks.com/help/gads/index.html>. [Accessed 2015 03 19].